Multiscale modeling of interaction of alane clusters on Al(111) surfaces: A reactive force field and infrared absorption spectroscopy approach

ARTICLE *in* THE JOURNAL OF CHEMICAL PHYSICS · FEBRUARY 2010

Impact Factor: 2.95 · DOI: 10.1063/1.3302813 · Source: PubMed

8 AUTHORS, INCLUDING:

J. G. O. Ojwang
Virginia Commonwealth University
17 PUBLICATIONS **93** CITATIONS
SEE PROFILE

Adri C.T. van Duin
Pennsylvania State University
360 PUBLICATIONS **8,049** CITATIONS
SEE PROFILE

William A. Goddard
California Institute of Technology
1,329 PUBLICATIONS **67,304** CITATIONS
SEE PROFILE

Multiscale modeling of interaction of alane clusters on Al(111) surfaces: A reactive force field and infrared absorption spectroscopy approach

J. G. O. Ojwang,[1,a)] Santanu Chaudhuri,[2] Adri C. T. van Duin,[3] Yves J. Chabal,[4] Jean-Francois Veyan,[4] Rutger van Santen,[5] Gert Jan Kramer,[5] and William A. Goddard III[6]
[1]*Geophysical Laboratory, Carnegie Institution of Washington, 5251 Broad Branch Rd. NW, Washington, DC 20015, USA*
[2]*Applied Sciences Laboratory and Institute for Shock Physics, Washington State University, Spokane, Washington 99210-1495, USA*
[3]*Department of Mechanical and Nuclear Engineering, Pennsylvania State University, University Park, Pennsylvania 16802, USA*
[4]*Department of Material Science and Engineering, University of Texas at Dallas, Richardson, Texas 75080, USA*
[5]*Schuit Institute of Catalysis, Eindhoven University of Technology, Postbus 513, 5600 MB, Den Dolech 2, Eindhoven, The Netherlands*
[6]*Materials and Process Simulation Center (MSC), California Institute of Technology, 1200 East California Boulevard, Pasadena, California 91125, USA*

(Received 20 November 2009; accepted 5 January 2010; published online 24 February 2010)

We have used reactive force field (ReaxFF) to investigate the mechanism of interaction of alanes on Al(111) surface. Our simulations show that, on the Al(111) surface, alanes oligomerize into larger alanes. In addition, from our simulations, adsorption of atomic hydrogen on Al(111) surface leads to the formation of alanes via H-induced etching of aluminum atoms from the surface. The alanes then agglomerate at the step edges forming stringlike conformations. The identification of these stringlike intermediates as a precursor to the bulk hydride phase allows us to explain the loss of resolution in surface IR experiments with increasing hydrogen coverage on single crystal Al(111) surface. This is in excellent agreement with the experimental works of Go *et al.* [E. Go, K. Thuermer, and J. E. Reutt-Robey, Surf. Sci. **437**, 377 (1999)]. The mobility of alanes molecules has been studied using molecular dynamics and it is found that the migration energy barrier of Al_2H_6 is 2.99 kcal/mol while the prefactor is $D_0=2.82\times10^{-3}$ cm^2/s. We further investigated the interaction between an alane and an aluminum vacancy using classical molecular dynamics simulations. We found that a vacancy acts as a trap for alane, and eventually fractionates/annihilates it. These results show that ReaxFF can be used, in conjunction with *ab initio* methods, to study complex reactions on surfaces at both ambient and elevated temperature conditions. © *2010 American Institute of Physics*. [doi:10.1063/1.3302813]

I. INTRODUCTION

The overarching aim of this study is to show that reactive force field (ReaxFF) can be used to model surface dynamics and reactions, with a focus on the interaction of alane molecules with Al(111) surface. We have chosen to study the interactions of alanes on Al(111) surface for the following four reasons: (i) we already have a well parametrized force field that aptly describes aluminum and aluminum hydride systems,[1] (ii) we have reactions of alanes in the gas phase and so it is worthwhile to make a comparison between the gas phase dynamics and surface reactions,[1] (iii) alanes are believed to be the ubiquitous facilitators of mass transport of aluminum atoms during the thermal decomposition of $NaAlH_4$, which is a potential hydrogen storage material,[2–5] and (iv) alanes also take part on decomposition of AlH_3, another important material for hydrogen storage.

In a previous publication, we showed that in the gas phase there is agglomeration-induced desorption of molecular hydrogen.[1] That is, the alane molecules first of all agglomerate/oligomerize before the desorption of molecular hydrogen occurs. In the light of these results, one might wonder if the same scenario (agglomeration) is mirrored in the condensed phase. In other words, how do clusters of AlH_3 behave on the surface of aluminum? Several experimental studies based on deposition of atomic hydrogen on aluminum surface have been conducted by various groups.[6–12] In some of these studies it was found that alanes were formed and then oligomerized. The oligomerization process was dependent on surface coverage, surface morphology, and temperature. In their study, Go *et al.*[9] observed that on the vicinity of steps the alanes oligomerized into long strings. Hara *et al.*[10] showed, using thermal desorption spectroscopy, that AlH_4, AlH_3, AlH, and AlH_2 species were desorbed from 0.5 ML H/Al(111) surface at 330 K, which was heated at a rate of 10 K/s. In their study, Hara and coworkers dosed atomic hydrogen on Al(111) surface and noted that all of adsorbed species desorbs at around 340 K as

a)Electronic mail: jojwang@ciw.edu.

aluminum hydrides such as AlH_3 or Al_2H_6. However, this happened at a ramping rate above 10 K/s. At low heating rates, and at 340 K, only molecular hydrogen is desorbed. This suggests that the adsorbed species are unstable and continuously undergo disproportionation to aluminum and molecular hydrogen.[10,13] In the experimental work of Herley *et al.*[11] they mentioned the formation of "small clusters of agglomerated lumps on reacted surface" during the thermal decomposition of AlH_3. Using energy dispersive spectroscopy scans they detected aluminum as the only metal present in the aggregate. One possibility is that the aggregate formed was aluminum oxide. However, this seems remote since aluminum oxide should have passivated the surface yet the decomposition process at 150 °C was accelerated by the presence of the aggregates. The other possibility is that these clusters were purely made up of aluminum atoms. However, the formation of more aluminum should have led to a slow rate segment as discussed in Ref. 14. Based on our present results, we suggest that these aggregates might have been alane clusters. Chaudhuri *et al.*[12] showed, using experimental Fourier transform infrared (FTIR) spectroscopy data, the coexistence of several adsorbed species on Al(111) surface. The relative concentration of these species was shown to be dependent on the roughness of the surface, surface coverage, and the temperature. Moreover, maturation of hydrogen storage technologies will require realistic regeneration routes for aluminum based hydrides. In this regard, agglomeration of aluminum hydride clusters leading to the growth of bulklike AlH_3 phase is critically important. The current study links the diffusion and oligomerization processes to initiation events leading to growth of a highly disordered hydride phase. Ongoing experimental and theoretical studies will be an important step in identifying possible pathways for the promotion of such growth under more ambient regeneration conditions than currently possible.

II. METHODS

A. Theoretical methods

ReaxFF is increasingly becoming a powerful tool for simulating chemical reactions. It has already been shown that ReaxFF provides a reliable description of the bulk properties, surface, and cluster properties of both aluminum[15] and aluminum hydride.[1] During the MD simulation atomic charges were updated per every iteration. This dynamical charge transfer allowed for fluctuations of atomic charges depending on the coordination of the atom. The parametrizations procedure of ReaxFF using density functional theory (DFT) derived data has already been discussed in Refs. 1, 15, and 16. In ReaxFF's simulations, in all cases unless stated otherwise, an aluminum slab with dimensions (28.6×24.75) was used. The slab was made up of five layers. Each layer had 100 atoms giving a total of 500 atoms. A vacuum equivalent to 20 layers was used in the z direction, which more than suitably separated the slab system from its periodic images. The total energy calculations based on DFT were carried out using the Vienna *ab initio* simulation package (VASP). In VASP the electron-ion interaction is described by projector augmented wave method. A cutoff energy of 450 eV (1 eV $=23.06$ kcal/mol) was used for the plane-wave basis set. A convergence of 10^{-6} eV/atom was placed as a criterion on the self-consistent convergence of the total energy. For the slab calculations in VASP, we used a three layer of aluminum slab with a total of 48 aluminum atoms. The slab was well separated from its periodic image by 10 Å of vacuum. Brillouin zone integrations were performed using a $9\times9\times1$ Monkhorst–Pack grid. The exchange-correlation energies were incorporated using the Perdew–Wang (PW91) version of the generalized gradient approximation. The isolated Al atom and the hydrogen molecule were modeled in a $15\times15\times15$ Å^3 cell using a cutoff energy of 450 eV. The molecular dynamics (MD) calculations were done using a velocity Verlet algorithm[17] to integrate Newton's equations of motion. The simulations were performed in the canonical ensemble, NVT (constant number of particles, volume, and temperature). The time step used for all simulations was 0.25 fs. This led to stable dynamics trajectories.

B. Experimental methods

The experiments were performed on $2.5\times1.0\times0.2$ cm^3 commercially produced Al(111) single crystal with one face mechanically and electrochemically polished. The sample, mounted on a $3.8\times1.5\times0.1$ cm^3 tungsten plate, was introduced in a UHV chamber with a base pressure of 2×10^{-10} Torr. The Al crystal was subjected to several cycles of 30 min Ar+ sputtering (500 eV) and annealing up to 400 °C, for a total time of approximately 20 h. The crystalline order and cleanliness of the surface were monitored both by using *in situ* low energy electron diffraction (LEED) and Auger emission spectroscopy (AES). The IR reflection absorption spectroscopy[12] (IRRAS) was performed using a midinfrared modulated beam generated by a thermo Nicolet Fourier transform interferometer specially adapted to operate in the Torr range of pressure. After reflection on a parabolic mirror, the IR beam was focused on the Al crystal surface with a glancing angle of 7° through a KBr window. After reflection from the sample surface, the beam exiting the chamber through another KBr window was refocused on a deuterated triglycine sulfate (DTGS) infrared detector. The IRRAS system, from the IR source to the entrance KBr window, was maintained under vacuum of around 10 Torr. The exit ellipsoidal mirror and the detector were maintained in a dry N_2 atmosphere.

The temperature of the sample was controlled by a combination of liquid nitrogen cooling and indirect heating using a Ta filament on the back of the W sample holder, and measured using a K-type thermocouple directly in contact with the sample. The temperature range can be varied from 90 to 800 K. For atomic H exposures, the experimental chamber was filled with molecular hydrogen. The hydrogen pressures in the range of 1×10^{-6} Torr was monitored by an uncorrected reading of the ion gauge before dosing. A 1.5 cm tungsten filament placed 8 cm from the Al surface and held at 2000 K dissociates the molecular hydrogen. The ion gauge was turned off during dosing. In our setup, the surface saturation for a sample temperature of 90 K, measured to be 1.6 ML by previous temperature programmed desorption (TPD)

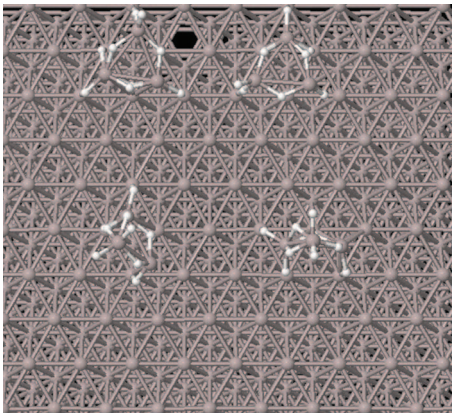

FIG. 1. Snapshots of four Al_3H_9 being adsorbed on Al(111) surface. Both the aluminum slab and the alanes were kept at a temperature of 300 K throughout this simulation run.

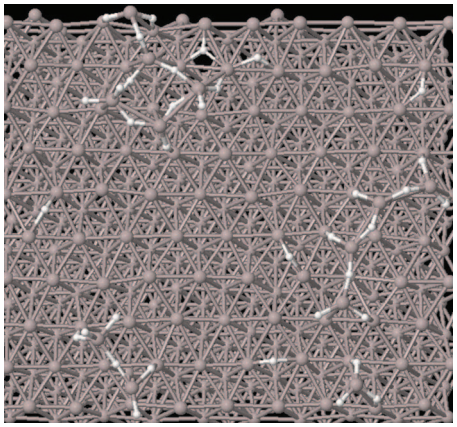

FIG. 2. Oligomerization of smaller alanes (Al_3H_9) into a large alanes at 800 K on Al(111) surface. The calculated agglomeration energy is −6.56 kcal/mol per AlH_3. Notice the stringlike conformation.

experiments (a H coverage greater than 1 ML is due to the formation of alanes), was reached at roughly 600 L. Assuming a linear dependence between exposure and coverage, we can therefore estimate that 1 L exposure leads to 0.3% of a monolayer. The temperature elevation of the sample due to the hot W filament (used to dissociate molecular hydrogen during dosing) is less than 1° for 15 s exposures and less than 10° for 600 s exposures.

III. RESULTS AND DISCUSSION

A. Alanes interaction on Al surface

In this section we discuss a number of theoretical models that were carried out in order to shed more light on the creation and growth of alanes, especially the work of Go *et al.*[9] There are three issues we set to iron out: (a) the details of the formation of alanes due to the interaction between atomic hydrogen and Al(111) surface, (b) the ordering and dynamical behavior of the formed alanes on Al(111) surface, and (c) the corrugation and reconstruction of the Al(111) surface after the formation and rearrangement of the alanes.

We have systematically performed a series of calculations to analyze the mechanisms in which alanes interact on Al(111) surface (strictly speaking alane refers to AlH_3 molecule but herein we shall refer to all the aluminum hydride complexes as alanes). In our first simulation, the temperature of the entire system was kept constant at 300 K. The system was first minimized and then equilibrated at 300 K for 50 000 time steps. The atomic configurations of the adsorbed alanes on the Al(111) surface are shown in Fig. 1. This snapshot of the atomic configurations was taken after 500 ps of simulation run.

At a temperature of 300 K the alanes are essentially immobilized on the Al(111) surface. They vibrate about their mean position but cannot diffuse due to the strong attachment to the substrate. Notice in Fig. 1 that two of the Al_3H_9 are vertically attached to the Al(111) surface while two are horizontally adsorbed. The reason for this is that alanes preferably approach Al(111) surface either vertically or in a slanting position so as to avoid direct Al–Al interaction. Once attached, the alanes then adopt a horizontal conformation. In our starting configuration all four Al_3H_9 were in vertical position. So the figure essentially shows that two of the Al_3H_9 have already been chemisorbed while the other two are being adsorbed.

We next inspected the mobility of the adsorbed alanes on Al(111) surface. The initial atomic configuration was the same as that in Fig. 1. After minimization, the temperature of the system was quickly ramped up to 800 K and kept constant for 125 ps. One reason for ramping up the temperature to 800 K was to try and see if we could observe desorption of molecular hydrogen during the production stage. This is based on the work of Go *et al.*[9] who noted that there was a loss of smaller alanes to higher alanes and to desorption at temperatures above 360 K. The other reason was to accelerate the diffusion process of atomic hydrogen and the alanes on the metal surface. Figure 2 is a snapshot of the simulation run after 500 ps.

Our results point to oligomerization of alanes as being the means by which aluminum atoms are transported. This is illustrated in Fig. 2. In trying to understand the figure one should take into consideration the presence of periodic boundaries. At the beginning of the simulation (Fig. 1) we had four Al_3H_9. At the end of the simulation (Fig. 2) most of these alanes have oligomerized. There are also four hydrogen atoms and an alane molecule diffusing on the surface. The agglomeration process is quite complex. Apart from agglomeration, alanes can undergo fragmentation and then reagglomeration (see Ref. 1). This depends on the morphology of the surface (defects such as vacancies facilitate fragmentation of alanes) and the potential energy landscape. We define agglomeration energy as the energy difference between the system prior to and after agglomeration, i.e.,

$$E_{agglom} = E_c(\text{agglom.}) - E_c(\text{unagglom.}), \quad (1)$$

where E_{agglom}, E_c(agglom.), and E_c(unagglom.) are the agglomeration energy, the cohesive energy of the system after agglomeration, and the cohesive energy of the system prior to agglomeration, respectively. The calculated agglomeration is −78.83 kcal/mol. This translates to about −6.56 kcal/mol per AlH_3. To obtain the cohesive energies, we used quenched MD simulation to cool the structures in Figs. 1 and 2 to 0 K toward their local minima. To ascertain that our observations

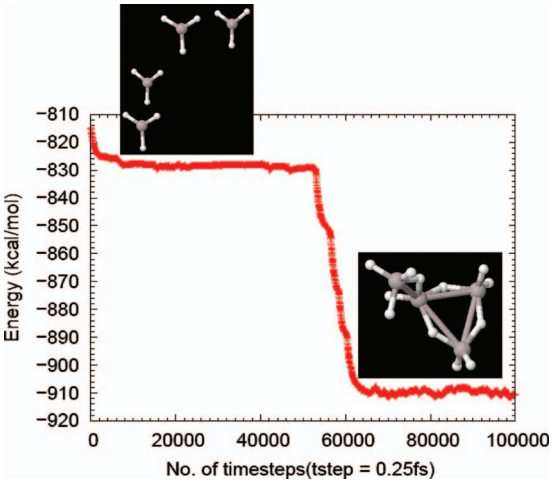

FIG. 3. Gas phase oligomerization of four alanes into a local minimum of Al_4H_{12}. The system exhibits drop in energy due to the exothermic nature of the oligomerization process. The calculated agglomeration energy is ca. −23.88 kcal/mol per AlH_3. This simulation run was conducted at 300 K.

are consistent with DFT, we simulated the agglomeration process of four alanes, in the gas phase, at 300 K. This is shown in Fig. 3. The calculated agglomeration energy for this process was already given in Ref. 1 (ca. −23.88 kcal/mol AlH_3). This is in excellent agreement with DFT value of −20.94 kcal/mol AlH_3. The DFT work was done at the PW91 level of theory in VASP. Using B3LYP level of theory with 6-311++G(d,p) basis set in GAUSSIAN03 program[18] we get an agglomeration energy of −28.86 kcal/mol AlH_3. In the DFT calculation we used the total energy of the most stable conformation of Al_4H_{12}. This is a cyclic structure with single bonds [see Fig. 4(a)]. We have previously shown (in Ref. 1) that the gas phase agglomeration of AlH_3 into $(AlH_3)_n$ polymeric units is exothermic by ca. −20 kcal/mol AlH_3 (at the PW91 level of theory). In an earlier work, Shen and Schaefer III[19] showed that the binding energy of Al_2H_6 relative to the monomer is in the range of −20.5 kcal/mol AlH_3 to −35.6 kcal/mol AlH_3, depending on the level of theory used. They obtained a value of −35.6 kcal/mol using double excitation coupled cluster method with double-zeta plus polarization basis sets. Our calculated value of agglomeration energy (binding energy of Al_4H_{12} relative to the monomers) is therefore within this range.

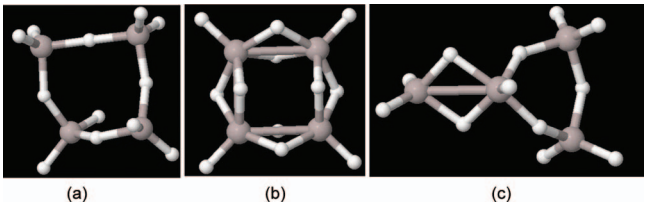

FIG. 4. The geometrical orientations of some of the possible isomers of Al_4H_{12}. In (a), singly bridged, all four aluminum atoms are tetrahedrally coordinated to hydrogen atoms. In (b), doubly bridged, all four aluminum atoms are coordinated to five hydrogen atoms. In (c), mixed singles and double bridges, three aluminum atoms are tetrahedrally coordinated to hydrogen atoms, and one Al atom is coordinated to five hydrogen atoms. Isomer (c) has not been reported in the literature before. The isomer was found by ReaxFF to be a local minima during MD simulation. It was then optimized in Gaussian at the B3LYP/6-311++G(d,p) level of theory. It was found to be stable and very close in energy to the singly bridged isomer (a).

We further optimized the Al_4H_{12} structure shown in Fig. 3 (herein referred to as quasicyclic) using the B3LYP exchange-correlation functional with 6-311++G(d,p) basis set. We then performed analytical vibrational frequencies analysis. The isomer was found to be stable (no imaginary frequency). The DFT computed dipole moment is 0.3 D, which is in perfect agreement with ReaxFF value of 0.302 D. The optimized geometry of the quasicyclic structure is shown in Fig. 4(c).

With zero point energy corrections included, the quasicyclic isomer is 2.54 kcal/mol less stable than the singly bridged isomer. The doubly bridged isomer lies significantly higher in energy by 25.2 kcal/mol relative to the singly bridged isomer. The highest-occupied molecular-orbital, lowest-unoccupied molecular orbital (HOMO-LUMO) gap for these three isomers is consistent with their relative energy differences. The gaps are −165.04, −128.64, and −161.27 kcal/mol for the single, double, and quasicyclic, respectively. The fact that ReaxFF could capture this quasicyclic structure, which is yet to be predicted in the literature, as a possible isomer of Al_4H_{12} demonstrates its versatility and predictive power as a tool for sampling the conformational phase space with a view to finding the possible local and global minima in chemical reactions.

Regarding Fig. 2, the formation of aluminum hydride complex strings is consistent with the experimental work of Go *et al.* where stringlike conformations in the vicinity of steps were seen. The oligomerization of alanes on Al(111) surface explains why there is a lack of coverage dependance of atomic hydrogen adsorption on Al(111) surface.[8] On the Al(111) surface, larger chemisorbed alane, starting with Al_2H_6, diffuse by reptation, i.e., snakelike motion. The diffusion mechanism of AlH_3 is quite complex. Since the AlH_3 is chemisorbed on the surface it is quite difficult for it to diffuse by shearing. The preferred mode of diffusion is leapfrog and summersault. In the leapfrog diffusion one of the diffusing atoms moves atop the AlH_3 molecule before settling in a different location. In the summersault scenario the AlH_3 slightly spins around its axis before the three H atoms settle in different locations but they are all still bonded to the same aluminum atom. Interestingly, we observed from a movie of the trajectories that a vacancy acts as an AlH_3 annihilation trap or rather aluminum atoms notoriously love each other. First, the AlH_3 is attracted and becomes attached at the vacancy. It then tries to flip over the vacancy. When the AlH_3 is on top of the vacancy, there is a strong metal-metal interaction between the Al atoms surrounding the vacancy and the Al atom in AlH_3. The Al atom (of AlH_3) becomes attached to the vacancy. This leads to self-healing of the Al(111) surface as illustrated in Fig. 5. The hydrogen atoms (having been stripped off of Al atom) then diffuse away.

The diffusion mechanism of AlH_2 is quite interesting. It seems as if it diffuses in a manner similar to someone rowing a boat. The aluminum atom moves forward and simultaneously the two hydrogen atoms move backward. In the next movement, as the two hydrogen atoms move forward the

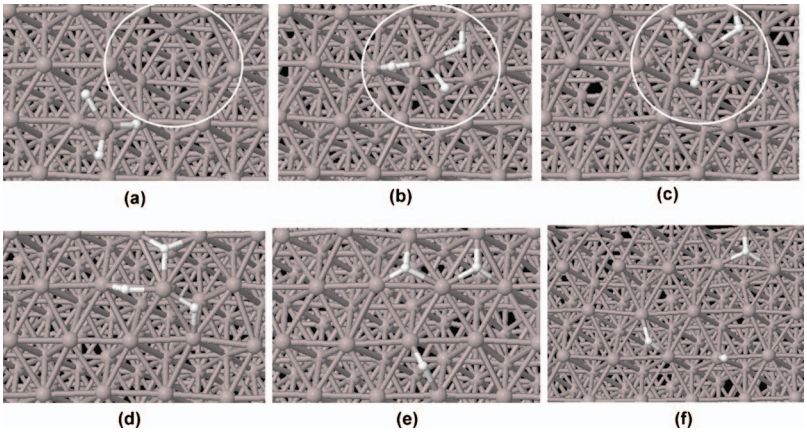

FIG. 5. Aluminum atoms notoriously love each other as shown by the fractionation of an aluminum hydride molecule by a vacancy. (a) AlH_3 approaching the vacancy. The vacancy is indicated by the white circle. [(b) and (c)] AlH_3 flips over and is trapped at the vacancy. (d) Surface aluminum atoms at the edges of the vacancy become attached to the Al atom in AlH_3. (e) The vacancy is repaired (self-healing) and (f) the hydrogen atoms diffuse away.

aluminum atom moves backward. The AlH_2 particle can also diffuse exotically by spinning around its axis with the two hydrogen atoms acting as wings. This interesting mechanism is akin to a bird flapping its wings as it flies in the air. To determine the correlation between the rate of diffusion and cluster size we next plotted mean square displacement (MSD) curves. Figure 6 shows the MSD curves of atomic hydrogen, AlH_3 and Al_2H_6 in the temperature range of 650–700 K. Surprisingly, our results show that AlH_2 has a low diffusivity compared to AlH_3. The reason for this is that the Al atom in AlH_2 is bonded to three surface Al atoms. This reduces its mobility since three Al bonds have to be cleaved for it to move. The diffusion of AlH_3, on the other hand is facilitated by the ability of one of the H atoms to leapfrog over the other atoms, which gives AlH_3 an extra degree of freedom compared to AlH_2. The preferred diffusion process of atomic hydrogen is to hop between the threefold hollow sites (fcc and hcp) via the bridge site. It intermittently also hops between the threefold site via the top site. However, this seems to cost more energy and as such can be considered as a rare event with respect to bridge site as a pathway.

The diffusion of atomic hydrogen and alane species (AlH_2, AlH_3, and Al_2H_6) over the temperature range of 600–725 K not only depends on the temperature (assuming the surface morphology remains the same) but is also highly susceptible to the nature of the potential energy surface. In other words, even at elevated temperatures, a species can get trapped in a local minima, which reduces its rate of diffusion. This is illustrated in Fig. 6, which shows the MSD of atomic hydrogen. In computing the MSD the system (slab +adsorbate) was heated up to the desired temperature (between 600 and 725 K) and equilibrated for 100 ps at this temperature. This was then followed by a production run for 25 ps in which diffusional analysis was performed. It can be seen in the figure that the MSD of atomic hydrogen at 675 K is larger than that at 700 K. To account for this discrepancy of the MSD from the expected temperature dependence we plotted the molecular simulation trajectories of atomic hydrogen at various temperatures as illustrated in Figs. 7 and 8.

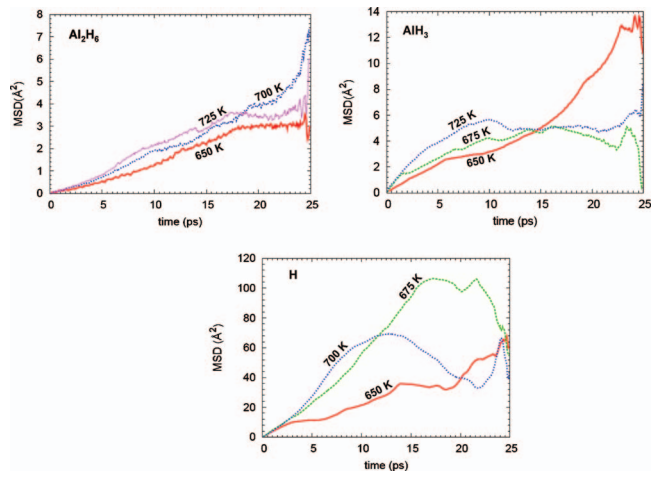

FIG. 6. The mean square displacements, $\langle \Delta r^2 \rangle$, of atomic hydrogen and mass-centers of AlH_3 and Al_2H_6 at different temperatures.

At 650 K the hydrogen atom oscillates between the local minima, which are the threefold hollow sites (fcc and hcp). At 675 and 700 K the hydrogen atom diffuses over a wider surface area since it has the requisite activation energy needed to move away from the local minima. The multidimensional nature of this potential energy surface at 675 K is illustrated in Fig. 8. The figure shows that the hydrogen atom gets trapped in particular conformations represented by the valleys (threefold sites) in the figure and occasionally diffuses over the hills (bridge and top sites). In fact as can be seen in Fig. 8(b) the hydrogen atoms hop between the threefold sites via the bridge and top site. This behavior was also seen in the case of AlH_2, AlH_3, and Al_2H_6. Most important, starting from a different configuration it was found that the MSD was temperature dependent as illustrated in Fig. 6 for the case of Al_2H_6. The diffusion coefficient for atomic hydrogen and the center of mass diffusion coefficients at a

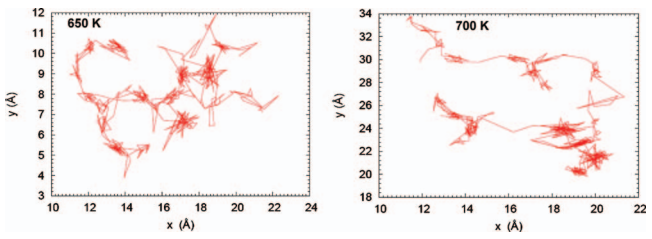

FIG. 7. MD simulations trajectories of atomic hydrogen on Al(111) surface at 650 and 700 K. At 650 K the hydrogen atom hops between the threefold hollow sites via the bridge site. At 700 K the hydrogen atom not only hops between the threefold sites but also diffuses much faster over a wider surface area.

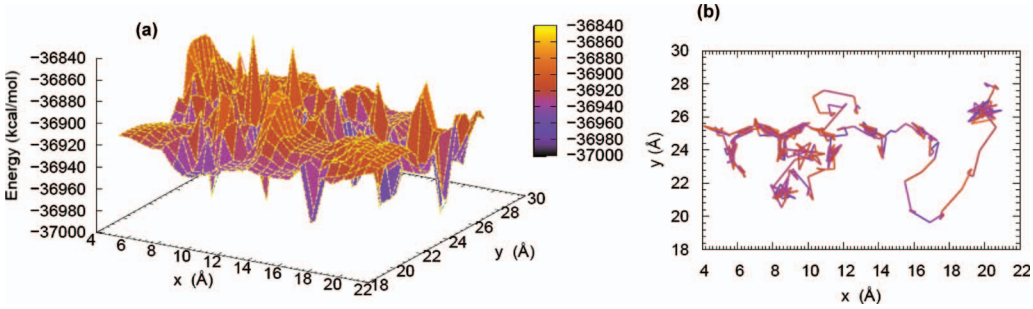

FIG. 8. (a) The complex energy landscape with deep valleys and mountains spanned by x and y coordinates of the diffusing hydrogen atom at a temperature of 675 K. (b) The trajectory of atomic hydrogen at 675 K.

given temperature for AlH_2, AlH_3, and Al_2H_6 were calculated from the simulation data using the Einstein relation,

$$D = \lim_{t\to\infty} \frac{\langle \Delta r^2(t) \rangle}{2dt}, \tag{2}$$

where d is the dimensionality of the system. For our case d =2 since motion along the vertical direction is frustrated. $\langle \Delta r^2(t) \rangle$ is the MSD of the mass center of cluster and is given by

$$\langle \Delta r^2(t) \rangle = |\Delta x^2(t) + \Delta y^2(t)|, \tag{3}$$

with $t=t_0+\Delta t$. Reasonable statistics to compute MSD is obtained by averaging $|\Delta x^2(t)+\Delta y^2(t)|$ over a number of time origins. The diffusion energy barrier E_a can be obtained using Arrhenius law for diffusivity

$$D = D_0 \exp\left(\frac{-E_a}{k_B T}\right). \tag{4}$$

It should be noted that in calculating the diffusion constant only the linear part of Fig. 6 was taken into account since if D is to be a constant then a plot of MSD versus time should be linear. The diffusion coefficient can be obtained from the long time behavior of MSD. We restricted our diffusion analysis to the temperature range of 600–725 K because above 750 K the dialane fragments into AlH_3 and other smaller species (AlH and AlH_2) while below 500 K its diffusion is not interesting, that is, it is almost immobilized. The migration energy barrier for Al_2H_6 and the prefactor, D_0, were computed using a linear regression analysis of D as a function of 1/T. The calculated prefactor is $D_0=2.82 \times 10^{-3}$ cm^2/s, while the migration energy barrier was found to be 2.99 kcal/mol. We could not compute the migration energy barrier of AlH_3 due to nonlinearity of the MSD as shown in Fig. 6. The cause of the nonlinearity of the MSD is surface trapping effects, which emanate from complex nature of the potential energy surface as illustrated in Fig. 8.

In experiments, usually atomic hydrogen is deposited on aluminum surface.[8,10,11] Complementary scanning tunneling microscopy and surface infrared (IR) measurements show that H reacts strongly with Al(111), producing a variety of new alane (aluminum hydride) surface species.[9] Figure 9 is an illustration of what happens when atomic hydrogen impinges on Al(111) surface. The figure shows that when atomic hydrogen are deposited on Al(111) surface they extract aluminum atoms from the surface, forming alanes. The formed alanes then oligomerize.

In order to investigate the etching of aluminum from the surface, the formation and subsequent dynamics of alanes on Al(111) surface, we used the work of Go *et al.* as a benchmark for modeling the interaction of atomic hydrogen with Al(111) surface. To do this, we placed atomic hydrogen (adatoms) on the top site of Al(111) surface. In this initial configuration, the hydrogen atoms were bonded terminally to aluminum atoms and inclined to the surface normal. If we define the surface coverage as the ratio of actual surface coverage of adsorbed species to that of saturation coverage (of surface atoms) then we have a monolayer coverage (1 ML). Interestingly, in our simulations, we observed that hydrogen atoms extract aluminum atoms directly on impinging the surface regardless of whether there is a vacancy or not. The notion of direct extraction of aluminum atoms from the terraces by impinging atomic hydrogen was also noted by Go *et al.*[9] The etching and chemisorption of the hydrogen atoms during the minimization process result in the formation of aluminum vacancies and as a consequence the corrugation of Al surface. Since defects are sites of high reactivity some hydrogen atoms diffuse to these sites during the equilibration process. This results in the formation of more aluminum hydride complexes. The formation of aluminum hydride complex, in turn, leads to significant adsorbate induced reconstruction, which is driven by the strong adsorbate-substrate interaction.

Like in the previous simulations, the temperature of the system was quickly ramped up and held at 800 K. The equilibration process leads to rapid evolution of the population of alanes as the adsorbed hydrogen atoms etch aluminum atoms to form alanes. At this high temperature there is significant

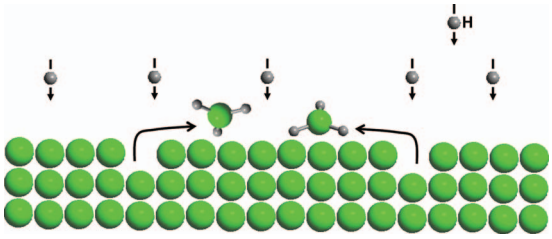

FIG. 9. Schematic representation of the deposition of atomic hydrogen on Al(111) surface. The hydrogen atoms etch aluminum atoms from the surface leading to the formation of alanes.

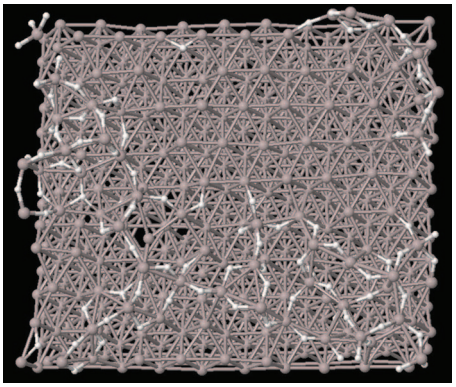

FIG. 10. (Top view) A snapshot from MD simulations. Oligomerization of the alanes to form an aluminum-hydride complex. At the middle of the aluminum surface we have an almost perfect Al(111) terrace instead of being corrugated or having atomic vacancies as one would expect. This surface is surrounded by an alanes complex. The formation of the flat terrace is due to reconstruction of the Al(111) surface.

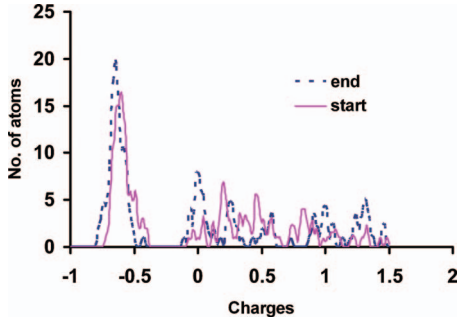

FIG. 11. Charge distributions of the aluminum atoms on the top layer of the slab plus the adsorbed hydrogen atoms, after minimization and at the end of the equilibration run (125 ps). The figure shows that at the end of the simulation there is a significant increase in the number of aluminum atom with charge of approximately 0. At the same time there is also an increase in the number of aluminum atoms with charges between +1 and +1.5.

thermal harvesting of alanes. The alanes oligomerize and the cluster grows. This leads to the formation of what we can term as aluminum hydride complex islands. This is illustrated in Fig. 10, which shows a top view of the structure at the end of the simulation run (125 ps). What the figure shows is that at the middle of the aluminum surface we have an almost perfect Al(111) ordering instead of being corrugated or having atomic vacancies as one would expect. This surface is then surrounded by an alanes mound. This is quite interesting because in the initial setup, after energy minimization, the surface was highly corrugated due to the formation of aluminum hydride and the etching of aluminum atom from the Al(111) surface by atomic hydrogen. This means that there must be some sort of reordering of the Al surface leading to the creation of a perfect (111) surface. We can attribute this restructuring to two factors. (a) There is a thermally activated vacancy migration. These vacancies then aggregate near the step edge. (b) There is the dissociation of alanes at aluminum vacancy sites. In other words, some aluminum atoms from alanes are captured back by some of the vacancies. The vacancy is then sealed (self-repaired) using these atoms. These deductions are based on our observation of the time evolution of the atomic trajectories during the molecular simulations run. Based on our definition of agglomeration energy in Eq. (1), the calculated agglomeration energy is −299.9 kcal/mol. However, we need to note that in this case there is an interplay of etching of aluminum atoms, formation of alanes, agglomeration of alanes, and surface reconstruction. Nonetheless from this number we see that the energy cost associated with the cleaving of aluminum bonds is adequately compensated for by the formation of alanes, agglomeration of alanes, and surface reconstruction.

To more fully understand the changes in chemical bonding due to agglomeration we plotted changes in charge distribution at the beginning and at the end of simulation. This is illustrated in Fig. 11. The figure shows the charge distributions of the aluminum atoms on the top layer of the slab plus the adsorbed hydrogen atoms, after minimization and at the end of the equilibration run. It can be seen in the figure that at the end of the simulation there is a significant increase in the number of aluminum atom with charge of approximately 0. At the same time there is also an increase in the number of aluminum atoms with charges between +1 and +1.5. We can interpret this observation as follows. As a result of reconstruction some of the aluminum atoms are reabsorbed back onto the aluminum surface. These are the aluminum atoms whose charge tends toward 0 as illustrated in Fig. 11. The aluminum atoms whose charge increase to the higher numbers belong to the alane oligomers. Notice in Fig. 11 that there is also a significant increase in charges of hydrogen atoms due to oligomerization and formation of the aluminum hydride complex.

B. Coverage dependent changes in infrared spectrum

The FTIR results point to a complex system where several adsorbed species coexist on the surface of the Al(111) single crystal. Their relative concentration and rate of formation depend on the step density, the surface coverage, and the sample temperature. Figure 12 shows a set of IR spectra from a stepped Al(111) surface for different hydrogen exposure at 90 K. For a 15 L exposure to atomic hydrogen (i.e., 15 s of H_2 gas at 10 Torr), the absorbance spectrum presents a strong IR band at 1795 cm^{-1}, with a small peak around 1860 cm^{-1}. With increasing the coverage to 75 L, this second sharp peak grows and blueshifts to 1874 cm^{-1}, while the 1795 cm^{-1} band broadens. They have been associated with vibration modes of AlH_3 at step edge (1795 cm^{-1}) and on terrace (1874 cm^{-1}). For coverage of 135 L, which represent 25% of a monolayer of H, a shoulder in the higher wave number region around 1900 cm^{-1} and a broad feature centered around 1600 cm^{-1} is growing. At saturation, above 540 L, the IR absorption spectrum presents broad feature in the 1500–1800 cm^{-1} frequency range and a sharper feature between 1800 and 2000 cm^{-1}. On the flat Al(111) surface, not shown here, the situation is somewhat different. For a 15 L exposure, there is no feature at 1795 cm^{-1}, but a mode centered at 1870 cm^{-1}. With increasing coverage, it appears that the spectra are composed of a broadened version of the three main features described previously for the stepped surface, and that these features grow simultaneously. Since the over-

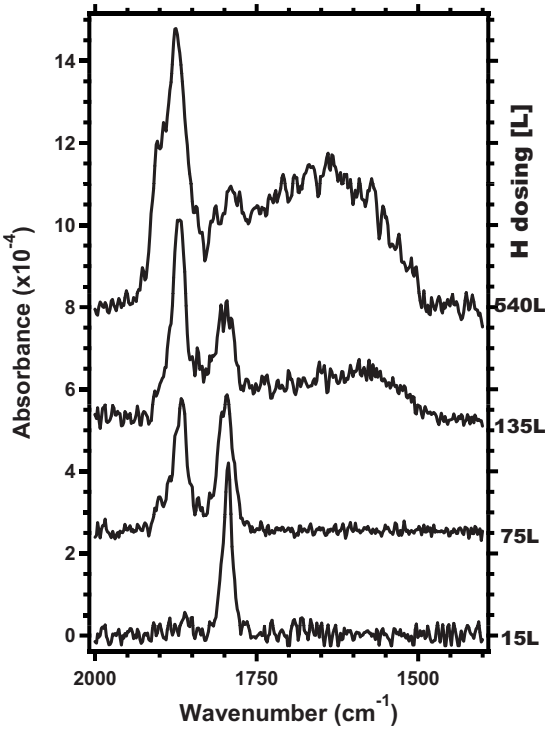

FIG. 12. Surface IR spectra from Al(111) surface after sequential dosing of hydrogen on a stepped Al(111) surface at 90 K at 1×10^{-6} Torr as indicated on the right side. The vibration modes become broad at higher surface coverage. This is due to oligomerization of alane clusters and their minimal surface attachment leads to averaging of net perpendicular surface dipoles.

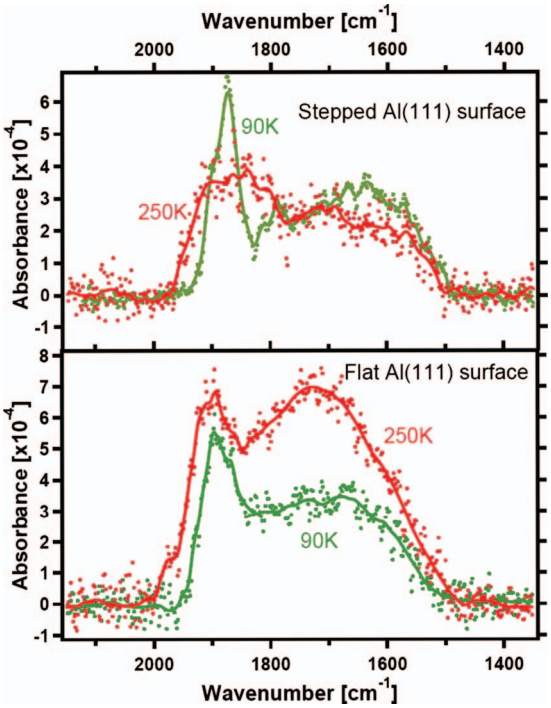

FIG. 13. The surface IR spectra from Al(111) surface after hydrogen saturation dosing at 90 K (green curve) and 250 K (red curve). Top: on a stepped surface; Bottom: on a flat surface. Dots indicate the experimental data, plain lines are fit.

all spectrum is much broader, it is not possible anymore to distinguish between the peak at 1874 cm^{-1} and the high-wave number shoulder.

Figure 13 summarizes IR experimental results from hydrogen saturated stepped Al(111) surface on top, and flat Al(111) surface on bottom, for two different temperatures. At 90 K, the spectra are quite similar. The IR data from the stepped surface present a higher intensity for the vibrational mode at 1875 cm^{-1}, while the flat surface shows a broadening of this feature toward higher wave numbers, a feature that has been associated to physisorbed oligomers on terraces.[12] The total amount of oligomers produced appears slightly higher for the stepped surface. At 250 K, the two surfaces interact with atomic hydrogen in totally opposite ways. On the stepped surface, the 1870 cm^{-1} feature is now boarder and divided by two in intensity, and the oligomer region below 1800 cm^{-1} is flattened. This could be explained by a higher mobility of the small alanes, and more favorable conditions for physisorbed rather than chemisorbed species on the surface. The flat surface at 250 K presents similar features as 90 K, with some noticeable differences. The total amount of oligomers adsorbed on this surface is almost doubled. The feature at 1875 cm^{-1} is blue-shifted and new modes appear at higher frequency, as a shoulder. The time frame for FTIR experiments is orders of magnitude away from the femtosecond time scale of the simulations. Our experimental technique can access only steady states of the system. Nevertheless, the theoretical models (both DFT and classical ReaxFF simulations) considered in this study also show that there are many possible stable environments for hydrogen adsorption on an Al(111) surface, from single H to larger alanes.

A general trend for the calculated frequencies can be drawn from these models. The DFT calculated values indicate that the broadening of the features around 1600 cm^{-1} is an indication of higher density of Al–H–Al linkages in oligomers. The ReaxFF studies provide a further explanation of this phenomenon. The longer chains of alanes contain 12 such linkages with vertical component. At the same time, the rotation and reorientation of these relatively free chainlike (or ladderlike) alane clusters will continually reorient the average dipole perpendicular to the surface. As a result, this work provides a first plausible explanation on the loss of resolution of IR spectrum. Further analysis of calculated IR power spectrum is currently underway to shed more light on the reorientation and coupling of surface dipoles from absorbed alane chains. Furthermore, rough Al(111) surface with higher step density tend to promote growth of the broadened regions starting from a lower temperature (180 K). To reconcile the difference between the temperature scale in experimental and theoretical results presented here, we have to understand the large difference in the time scale. It is thus logical to assume that alane oligomerization observed by both techniques is real, however, the rate of this process still remains an important open question.

IV. DISCUSSION

We can infer the following from the MD simulations and FTIR results. When Al(111) surface is exposed to a flux of monoatomic H, the impinging H atoms etch aluminum atoms

directly from the surface leading to formation of smaller alanes (AlH, AlH_2, AlH_3, and Al_2H_6, among others). As a result of this, the Al surface becomes roughened/corrugated resulting in the formation of steps. Stepped surfaces act as good nucleation sites for the formation and growth of alanes. Since the alanes are instantaneously formed it implies that there is no kinetic barrier to their formation. Thus there is a thermal induced harvesting of small alanes. The small alanes agglomerate into large alanes since the latter have greater stability. During this agglomeration process, the surface morphology of the Al surface changes. The alanes oligomerize to form a stringlike conformation (or alane islands) at the steps while any existing vacancies at the terraces are repaired. The calculated diffusion constant for H, AlH_2, and AlH_3 at 675 K are 8.88×10^{-5}, 2.39×10^{-6}, and 6.25×10^{-6} cm^2/s, respectively. This shows that these small alanes are very mobile on the flat surface. Vacancies provides a barrier for diffusion of alanes or atomic hydrogen. Whereas AlH_3 is annihilated (fragmented) at the vacancy, the monoatomic H is trapped at the vacancy and forms a bound hydrogen-vacancy complex. In addition, upon adsorption, AlH_3 can fragment into AlH and AlH_2. Similarly Al_2H_6 can fragment into AlH, AlH_2, and AlH_3. However, these alanes again agglomerate into larger alanes. At very low coverage both small alanes and large alanes coexist (see Fig. 2). However, as the coverage increases there is a preference for the formation of larger alanes (see Fig. 10).

As shown in previous studies,[1] oligomerization process is an exothermic process so locally there is a rise in temperature. The local rise in temperature leads to Al–H bond dissociation. As a result of this, molecular hydrogen is desorbed from the oligomer. The desorption of molecular hydrogen is thus given by the process,

$$\underbrace{\tfrac{2}{3}AlH_3}_{\text{(oligomers)}} \rightleftharpoons \tfrac{2}{3}Al + H_2. \tag{5}$$

From our analysis, the implication on the thermal decomposition of $NaAlH_4$ is that alanes molecules are formed. These then agglomerate into larger alanes (oligomers) due entropy. Taking into account the formation and oligomerization of alanes, the decomposition pathway of $NaAlH_4$ is as follows:

$$NaAlH_4 \rightleftharpoons \tfrac{1}{3}Na_3AlH_6 + \underbrace{\tfrac{2}{3}AlH_3}_{\text{(oligomers)}} \rightleftharpoons \tfrac{1}{3}Na_3AlH_6 + \tfrac{2}{3}Al + H_2, \tag{6}$$

$$Na_3AlH_6 \rightleftharpoons 3NaH + \underbrace{AlH_3}_{\text{(oligomers)}} \rightleftharpoons 3NaH + Al + \tfrac{3}{2}H_2. \tag{7}$$

A. Interaction of atomic hydrogen with an aluminum vacancy

It is likely that the exposure of aluminum surface to H atom beam will generate a substantial number of vacancies and bound hydrogen-vacancies complexes. Our goal in this respect was to get a fundamental understanding on how the presence of a vacancy affects the mobility of diffusing hydrogen atoms and alane species. In particular, how are vacancies created? How do vacancies interact with atomic hydrogen and alanes? Is there vacancy-vacancy interaction on Al(111) surface? Do bound hydrogen-vacancy complexes interact with each other? This last question is particularly important since it will give us some ideas on how stepped surface are formed.

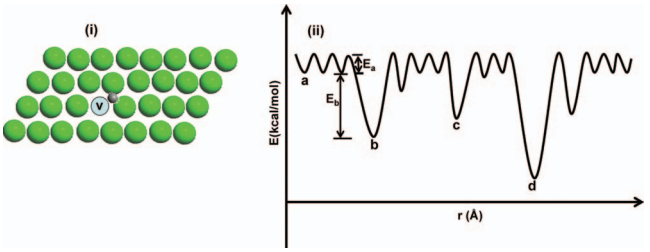

FIG. 14. Schematic diagram showing (i) a hydrogen atom trapped at the bridge site due to localized minimum on the potential energy surface of this site. (ii) Potential energy diagram of the Al(111) surface, site b represents the potential energy well where the hydrogen atom is trapped in. Site d might be the bridge site with double vacancies. E_a is the migration energy barrier and E_b is the binding energy of the vacancy. The binding energies for site b are −5.23 and −1.01 kcal/mol using ReaxFF and DFT, respectively.

In their work, Go and co-workers noted that it is possible that mobile atomic vacancies created during hydrogen adsorption may capture surface alanes and immobilize them on the substrate. From our simulations we have seen that, in addition, mobile atomic vacancies should fragment alane and use the aluminum in alane for self-repair. Larger alanes, however, can be captured and immobilized by the atomic vacancies. This leads to a reconstruction of the vacant site and eventual fragmentation of the trapped large alane. Interestingly, we observed a H-atom diffusing (hopping between bridge and hollow sites) toward and being trapped by a vacant site. This resulted in the formation of vacancy-hydrogen (Al_{vac}–H) complex/pair. This is because the vacancy is a local minima of the potential energy surface. This is schematically depicted in Fig. 14, which shows the various minima in the potential energy surface. Site a represents the chemisorption potential energy well on the flat Al(111) surface. It must be that these trapped atomic hydrogen are what were observed by Go and co-workers. What was actually very interesting in this simulation is that we observed the Al_{vac}–H pair diffusing as one entity. The binding energy of H at a vacancy is defined as

$$E_b = E_c(v+H) - E_c(v) - \tfrac{1}{2}E(H_2), \tag{8}$$

where $E_c(v+H)$ is the cohesive energy of slab+H+vacancy, $E_c(v)$ is the cohesive energy of slab+vacancy, and $E(H_2)$ is the total energy of molecular hydrogen (E_t= −156.87 kcal/mol). With this definition the calculated binding energies of atomic H to the vacancy is −5.23 and −1.01 kcal/mol using ReaxFF and DFT, respectively. It should be noted that we used the total energy of molecular hydrogen as our reference. Essentially, it costs energy to dissociate molecular hydrogen into atomic H, which then binds to the vacancy. If we use the total energy of atomic H (E_t= −25.79 kcal/mol) as our reference then the calculated (DFT) binding energy of H to the vacancy is −53.66 kcal/mol. A similar observation on the formation of vacancy-hydrogen

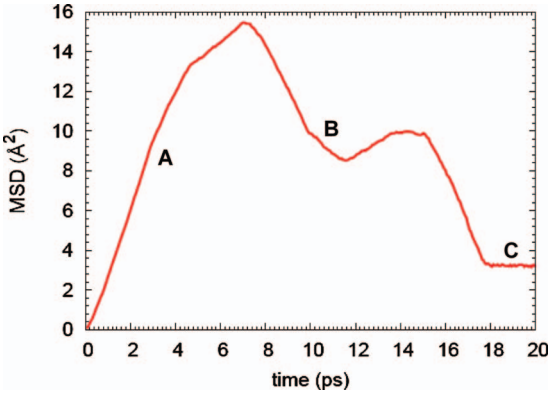

FIG. 15. The mean square displacement of atomic hydrogen attached to a vacancy at 675 K. Atomic H diffuses away but is again attracted to the vacancy. The first portion (region A) where there is dramatic increase in MSD is due to the hydrogen atom breaking free from the bound hydrogen-vacancy complex. It then diffuses about the surface. However, after some time it is attracted back to the vacancy. Region B represents that time frame where the hydrogen atom is attracted to the vacancy and slowly loses its mobility. In region C (where the MSD has a value of 3 $Å^2$) the hydrogen atom is vibrating about its mean position (Al–H–Al bridge) at the vacancy.

pair was noted by Hashimoto *et al.* in Ref. 20.

Figure 15 shows the MSD of the hydrogen atom attached to the vacancy at 675 K. Initially there is a rapid increase in the MSD with time to a peak value of 15.46 $Å^2$ at 7 ps. It then drops dramatically to a value of 3 $Å^2$ after 25 ps. The first portion of Fig. 15 (region A) where there is dramatic increase in MSD is due to the hydrogen atom breaking free from the bound hydrogen-vacancy complex. It then diffuses about the surface. However, after some time it is attracted back to the vacancy. Region B represents that time frame where the hydrogen atom is attracted to the vacancy and slowly loses its mobility. In region C (where the MSD has a value of 3 $Å^2$) the hydrogen atom is vibrating about its mean position (Al–H–Al bridge) at the vacancy. This simulation was conducted in the temperature range of 625–725 K. However, only at 675 K did the hydrogen atom break free from the vacancy, darted around, and reattached itself to the vacancy. For all the other temperatures the atomic hydrogen did not break free from the hydrogen-vacancy complex.

1. Further work

As part of further studies we intend to use kinetic Monte Carlo simulations to examine the rate of oligomerization of smaller alanes. One important modeling study that we are pursuing is to dope Al surface with Ti and study the effect of this on the rate of oligomerization of alanes, molecular hydrogen absorption/dissociation on Al surface, and its release from Al surface at higher coverage of alanes.

V. CONCLUSION

We have shown that ReaxFF can be used for simulating dynamical processes and as a computational tool to explore reactions of molecules with metal surfaces, which is an important area in catalysis. We have confirmed, using ReaxFF, that smaller alanes agglomerate into larger alanes. On Al(111) surface, the alane molecules can be formed by the hydrogen atoms, which directly extract Al atoms upon impinging the Al surface. Qualitatively our results strongly support the experimental works of Fu *et al.*[5] and Go *et al.*,[9] who have shown the existence of alane species. In particular, Go *et al.* have shown that small alane clusters do agglomerate to form large clusters but added that experimental limitations might hinder the observation of compound aluminum hydride clusters. From atomistic simulations we have shown (seen) that atomic hydrogen are attracted to vacancies and so are alanes. Aluminum hydride molecule (AlH_3) is easily annihilated by a vacancy. Larger alanes also get attached to vacancies but due to their relatively larger sizes they are not destroyed by vacancies. For these larger alanes vacancies can be effectively treated as steps, which act as seeds for alane clusters growth. A consequence of this is that on a corrugated surface, where there are many steps, there is the likelihood of not only oligomerization but also fragmentation of mobile alane species.

ACKNOWLEDGMENTS

This work is part of the research programs of Advanced Chemical Technologies for Sustainability (ACTS), which is funded by Nederlandse Organisatie voor Wetenschappelijk Onderzoek (NWO). J.G.O.O. thanks Jason Graetz, Geert Jan Kroes, and Andreas Züttel for fruitful discussion on agglomeration process of alanes during the MH2008 conference in Iceland. S.C. acknowledges ONR Grant No. N00014-03-1-0247. Y.J.C. acknowledges Hydrogen Fuel Initiative Award (Grant No. BO-130) of the U.S. Department of Energy and supported by Division of Chemical Sciences, Office of Basic Energy Sciences.

[1] J. G. O. Ojwang, R. van Santen, G. J. Kramer, A. C. T. van Duin, and W. A. Goddard III, J. Chem. Phys. **131**, 044501 (2009).
[2] J. G. O. Ojwang, R. van Santen, G. J. Kramer, and X. Ke, J. Solid State Chem. **181**, 3037 (2008).
[3] R. T. Walters and J. H. Scogin, J. Alloys Compd. **379**, 135 (2004).
[4] S. Chaudhuri, J. Graetz, A. Ignatov, J. J. Reilly, and J. T. Muckerman, J. Am. Chem. Soc. **128**, 11404 (2006).
[5] Q. J. Fu, A. J. Ramirez-Cuesta, and S. C. Tsang, J. Phys. Chem. B **110**, 711 (2006).
[6] J. Paul, Phys. Rev. B **37**, 6164 (1988).
[7] A. Winkler, C. Resch, and K. D. Rendulic, J. Chem. Phys. **95**, 7682 (1991).
[8] H. Kondoh, M. Hara, K. Domen, and H. Nozoye, Surf. Sci. **287–288**, 74 (1993).
[9] E. Go, K. Thuermer, and J. E. Reutt-Robey, Surf. Sci. **437**, 377 (1999).
[10] M. Hara, K. Domen, T. Onishi, H. Nozoye, C. Nishihara, Y. Kaise, and H. Shindo, Surf. Sci. **242**, 459 (1991).
[11] P. J. Herley, S. O. Christofferson, and J. A. Todd, J. Solid State Chem. **35**, 391 (1980).
[12] S. Chaudhuri, S. Rangan, J. Veyan, J. T. Muckerman, and Y. J. Chabal, J. Am. Chem. Soc. **130**, 10576 (2008).
[13] A. Winkler, G. Poigainer, and K. D. Rendulic, Surf. Sci. **251–252**, 886 (1991).
[14] I. M. K. Ismail and T. Hawkins, Thermochim. Acta **439**, 32 (2005).
[15] J. G. O. Ojwang, R. van Santen, G. J. Kramer, A. C. T. van Duin, and W. A. Goddard III, J. Chem. Phys. **128**, 164714 (2008).
[16] S. Cheung, W. Deng, A. C. T. van Duin, and W. A. Goddard III, J. Phys. Chem. A **109**, 851 (2005).
[17] L. Verlet, Phys. Rev. **159**, 98 (1967).
[18] M. J. Frisch, G. W. Trucks, H. B. Schlegel *et al.*, GAUSSIAN 03, Gaussian Inc., Wallingford, CT, 2004.
[19] M. Shen and H. F. Schaefer III, J. Chem. Phys. **96**, 2868 (1992).
[20] E. Hashimoto and T. Kino, J. Phys F: Met. Phys. **13**, 1157 (1983).